Technical Notes

TECHNICAL NOTES are short manuscripts describing new developments or important results of a preliminary nature. These Notes cannot exceed 6 manuscript pages and 3 figures; a page of text may be substituted for a figure and vice versa. After informal review by the editors, they may be published within a few months of the date of receipt. Style requirements are the same as for regular contributions (see inside back cover).

Design of Axisymmetric Bodies with Minimum Transonic Drag

Cuong P. Nghiem* and Helge Norstrud†
Norwegian Institute of Technology
Trondheim, Norway

Introduction

THE use of area ruling, based on concepts developed by Oswatitsch and Keune[1] and Whitcomb,[2] to devise low-drag transonic configurations requires the knowledge of an equivalent body of revolution having minimum transonic wave drag. Several optimum slender axisymmetric bodies have been presented.[3-7] They are all local optimum since their appearance differs from one another as well as from the optimum body obtained experimentally.[8] From the results presented in Refs. 3-5, it may be concluded that 1) nose bluntness and finite base play a role in reducing the body transonic drag, 2) in the case of a general parabolic shape the transonic drag is a function of the location of maximum cross-section area (or nose bluntness), and 3) optimum bodies in transonic flows should have no surface pressure jump.

Unlike the preceding investigations, preliminary design is the matter of concern in this Note. We start with the typical bodies of revolution with pointed noses (Fig. 1) and decompose each body into a forebody and an afterbody. Then we show that 1) in the case of a general parabolic shape with midsection as maximum cross section, nose bluntness gives low body drag but not afterbody bluntness, 2) nose bluntness gives body drag reduction because it gives foredrag reduction, and 3) among the typical axisymmetric shapes considered, blunt ogive shapes give minimum wave drag at transonic speeds.

Approach

The approach of this investigation is to exploit the sonic independence of the forebody and afterbody flows so that the afterbody drag of different shapes can be compared; to exploit the Miles' sonic foredrag formula,[9] so that the foredrag can be approximatively decomposed into a subsonic drag for the body portion upstream of the sonic location and a supersonic drag for the portion between the sonic location and the maximum cross section; and to use the drag buildup to evaluate the drag of a body portion where the drag buildup is defined as

$$C_{BD} = \frac{1}{S_{\max}} \int_{\text{nose}}^{x} C_p(x) S'(x)\, dx \qquad (1)$$

Thus, the drag of the whole body is computed by surface pressure integration and the drag of a body portion is given from the difference between the values of C_{BD} at the portion's ends.

Some preliminary remarks can be made. The conical forebody shape is not interesting since it is well known that the foredrag of such a shape is a function of the cone angle. The cylindrical body portion carries no drag and thus the drag of body 6 in Fig. 1 is equal to the foredrag. For drag comparison purposes, all bodies investigated must have the same thickness ratio; for convenience, they are selected having the same maximum cross-section area and only smooth shapes are investigated since our analysis is based on transonic small perturbation theory. Therefore, only bodies 4-7 without the cylindrical midsection are investigated in this study. Note also that a symmetric fore- and aftbody at transonic speeds has a typical surface pressure distribution that is asymmetric and has a pressure jump. It is therefore convenient to decompose the transonic drag into a shock drag due to the presence of the surface pressure jump, and a wave drag due to the asymmetry of the surface pressure. The shock drag can be nullified by using inverse design with a smooth surface pressure distribution as target. Minimizing the wave drag is a more challenging problem.

All bodies are defined for $-0.5 \le x \le 0.5$. The general parabolic shape of a pointed body portion is described by[10]

$$R(x) = R_{\max}\left\{1 - 2\epsilon_1\left[1 - \sqrt{1 - \frac{\epsilon_1 - \frac{1}{4}}{\epsilon_1^2}(Ax + B)^2}\right]\right\} \qquad (2)$$

where $R_{\max}$ is the maximum body radius, ϵ_1 the shape parameter, and A and B parameters introduced for giving a unified

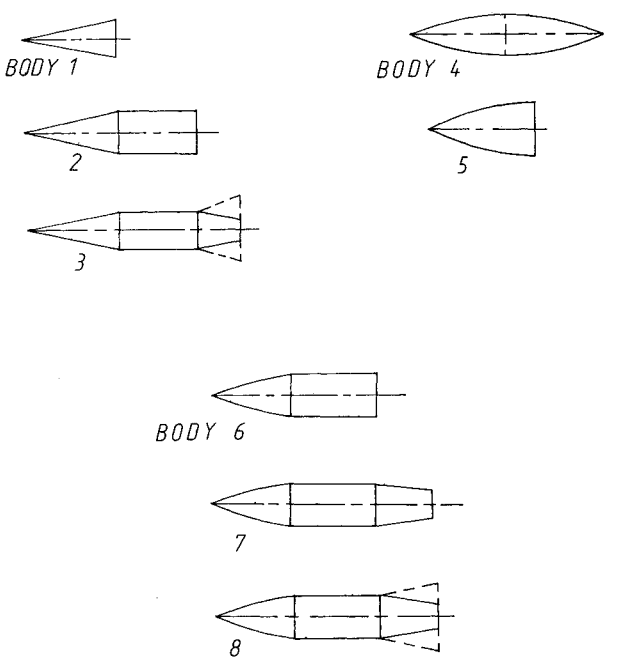

Fig. 1 Typical shapes of bodies of revolution with pointed noses.

Received Oct. 25, 1988; revision received March 24, 1989.

*Graduate Student, Division of Hydro and Gas Dynamics.
†Professor, Division of Hydro and Gas Dynamics. Associate Fellow AIAA.

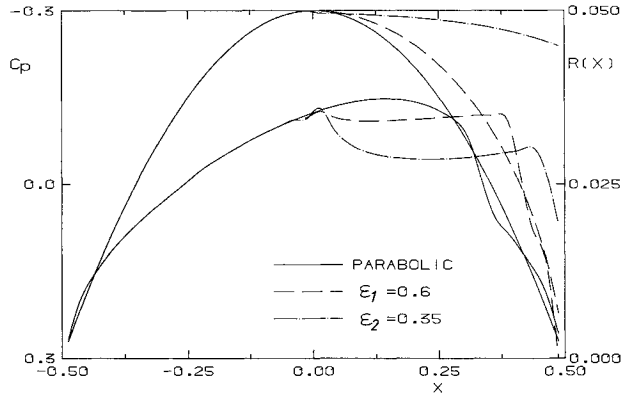

Fig. 2 Parabolic forebody with perturbations of parabolic and cylindrical afterbody.

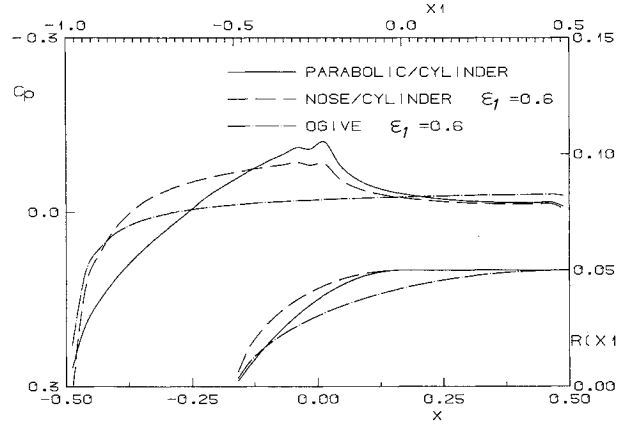

Fig. 3 Perturbations of parabolic forebody with cylindrical afterbody and parabolic ogive.

equation for both forebody, afterbody, and ogive shapes. For forebodies (Fig. 2) and afterbodies, $A = 2$, $B = 0$. For ogive shapes, $A = -1$, $B = 0.5$. Note that the forebody and the ogive shapes described by Eq. (2) satisfy the conditions of a pointed nose and zero slope at the maximum cross section required for application of the Miles' sonic foredrag formula. When ϵ_1 is very large, a parabolic body results. Blunt shapes are given by small values of ϵ_1. Note also that the Sears-Haack forebody or afterbody is a perturbation of the parabolic shape ($\epsilon_1 = 0.72$), but not the von Kármán ogive. However, they are both optimum shapes in linearized supersonic flow.

Conical afterbody shapes (Fig. 2) can be obtained by perturbing the cylindrical afterbody shape. These shapes can be described by

$$R(x) = R_{\max} \tanh\left(\frac{1-x}{\epsilon_2}\right) \tag{3}$$

where ϵ_2 is a shape parameter. More conical shapes are obtained with larger values of ϵ_2.

Results and Discussion

To investigate the role of bluntness of the parabolic afterbody, we keep the forebody parabolic and perturb the parabolic and the cylindrical afterbody shapes (Figs. 2 and 3). Note that if the design Mach number is not very close to unity, then a reshaping of the afterbody may require that the forebody must be reshaped too (see Fig. 12 in Ref. 3). The redesigned forebody thus gives a different foredrag. The difference between the initial and the new foredrag can be seen as an interference drag (interference between forebody and afterbody). In the present case, the afterbody flow has no influence on the forebody flow, there is no interference drag, and the drag of different afterbody shapes can then be compared. Results obtained show that the drag of perturbed parabolic afterbody shapes is nearly invariant, independent of the shock location.

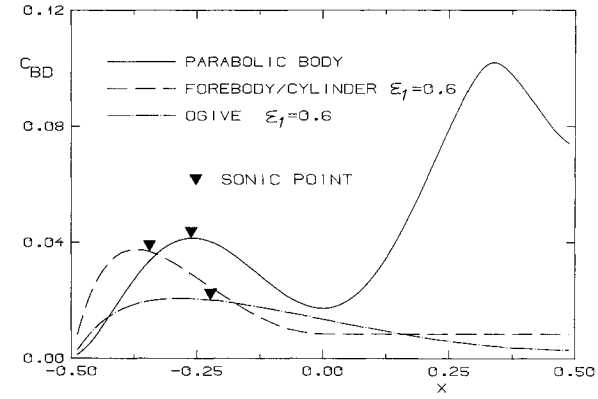

Fig. 4 Drag buildup of parabolic body, of body with blunt nose and cylindrical afterbody, and of blunt ogive.

In the case of perturbed cylindrical and conical afterbody shapes, we found that the surface pressure distributions are smooth, the flow decelerates smoothly at the junction section, and the more conical shape gives higher afterbody drag. We reach the same conclusion as in Ref. 4, in that the cylindrical afterbody gives lower drag than conical afterbodies because the body drag is reduced to the foredrag (Fig. 4).

To investigate the role of nose bluntness in drag reduction, we consider bodies with cylindrical afterbody and ogives. The foredrag of these bodies is a wave drag. The bodies investigated here are only moderately blunt and overexpansions at the nose resulting in a shock do not occur (see Fig. 9, Ref. 3). We also found that the location $S''(x) = 0$ is no longer a good approximation for the sonic location on the body surface when the nose is blunt. This can be attributed to a stronger influence of the nonlinear outer flowfield on the inner flowfield at a high degree of nose bluntness. In the case of a body with a cylindrical afterbody, the flow decelerates smoothly at the junction point. In the other case, the flow expands continuously over the ogive's surface (see Fig. 3).

From Fig. 4 it may be seen that the subsonic drag of a forebody results from a continuous increase in drag buildup and that the supersonic region gives less (supersonic) drag. The results show also that subsonic nose drag is proportional to the extent of the subsonic region near the nose. In general, the flow expands more rapidly compared to noses that are sharper. Here the extent of the subsonic region near the nose is smaller, so blunt bodies give less subsonic drag, and thus less body drag reduction. Therefore, for a given class of forebodies or ogives, blunt bodies give generally low body drag. From Fig. 4 it can also be seen that blunt ogives give the lowest sonic (fore) drag among the types of bodies investigated.

Conclusions

From the results presented, it may be concluded that an optimum body in transonic flow should have not only a smooth surface pressure distribution, but also a pressure distribution yielding minimum wave drag. If pointed bodies are of interest, a blunt body can be started with and then inverse design used to reshape the afterbody for a smooth surface pressure distribution. If infinite bodies (bodies fitted with sting) are of interest, transonic drag reduction can be achieved with a blunt forebody fitted with a cylinder. If bodies with a cylindrical base are of interest, a blunt ogive shape may be used since it gives low-wave drag at transonic speeds.

References

[1]Oswatitsch, K. and Keune, F., "Ein Aquivalensatz fur Nicht-tangestellte Fluge Kleiner Spannweite in Schallnaher Stromung," *Zeitschrift fur Flugwissenschaften,* Vol. 3, No. 2, Feb. 1955, pp. 29-46.

[2]Whitcomb, R. T., "A Study of the Zero Lift Design Drag Rise Characteristics of Wing-Body Combinations Near the Speed of Sound," NACA Report 1273, 1952.

[3]Malmuth, N. D., Wu, C. C., and Cole J. D., "Slender Body Theory and Optimization Procedures for Transonic Lifting Wing Bodies," *Journal of Aircraft,* Vol. 21, April 1984, pp. 256-263.

[4]Shankar, V., "Numerical Boundary Condition Procedure for the Transonic Axisymmetric Inverse Problem," NASA CP 2201, 1981, pp. 183-197.

[5]Chan, Y. Y., Mundie, D. L., and Jones, D. J., "Transonic Axisymmetric Bodies with Minimal Wave Drag," *Canadian Aeronautics and Space Journal,* Vol. 26, No. 3, 1980, pp. 231-234.

[6]Hassan, A. A., "A Method for the Design of Shock-Free Slender Bodies of Revolution," *AIAA Journal,* Vol. 24, May 1986, pp. 728-734.

[7]Burg, K. and Zierep, J., "Profile Geringsten Widerstandes bei Schallanstromung," *Acta Mechanica,* Vol. 1, 1965, pp. 93-108.

[8]Whitcomb, R. T., "Transonic Empirical Configuration Design Process," AGARD-R-712, 1983, pp. 8.1-8.9.

[9]Miles, J. W., "On the Sonic Drag of a Slender Body," *Journal of the Aeronautical Sciences,* Vol. 23, Feb. 1956, pp. 146-154.

[10]Krasnov, N. F., *Aerodynamics of Bodies of Revolution,* edited and annotated by D. N. Morris, American Elsevier, New York, 1970.

Sound Radiation from an Airfoil Encountering an Oblique Gust in Its Plane of Motion

Stewart A. L. Glegg*

Florida Atlantic University, Boca Raton, Florida

I. Introduction

SOUND radiation from airfoils that encounter oblique upwash gusts has been studied extensively, and many formulations[2-4] give the radiated field in terms of the unsteady lift fluctuations resulting from the interaction. When the airfoil encounters a gust in the plane of motion at zero angle of attack, there will be no upwash, and hence no unsteady lift. But, sound radiation will still occur due to the unsteady thickness noise components[1] that radiate sound when a blade of finite thickness encounters a velocity perturbation in the plane of motion. The purpose of this Note is to evaluate the radiated acoustic field and demonstrate its significance. However, the analysis does not include the effect of mean flow distortion on the gust.

The principal application of this analysis is considered to be the prediction of helicopter tail rotor noise. In this case the tail rotor is operating in the wake of the helicopter fuselage and hence, the blades will be moving in and out of the velocity deficit associated with the fuselage wake. This only has velocity components in the direction of flight, and hence the tail rotor will only experience unsteady flow components in the plane of motion.

The analysis is based on the unsteady thickness noise theory described in Ref. 1, and, as will be shown below, the sound radiation is dominated by the transient effect of the blade tip moving into the velocity deficit. Consequently, the effects of blade rotation are not important, and acoustic field can be obtained by considering a simplified model of a semi-infinite blade moving in rectilinear motion into the deficit (see Fig. 1). To apply the results to a helicopter tail rotor, the acoustic pulses generated by the blade tip moving in and out of the deficit are then summed at the correct retarded times and radiation angles relative to the observer.

Received Dec. 12, 1987; revision received March 16, 1989.

*Associate Professor, Department of Ocean Engineering.

II. Analysis

Consider an airfoil of semi-infinite span moving in rectilinear motion with velocity U, as illustrated in Fig. 1. The airfoil is initially assumed to be moving through a stationary fluid, before crossing a boundary into a region where the fluid is moving with velocity ΔV parallel to the boundary in the plane of motion. A set of blade-based coordinates y_1 are specified where y_1 lies in the chordwise direction and y_2 in the spanwise direction. The boundary of the moving fluid makes an angle Θ with the direction of blade motion. Finally, the observer position is specified in a set of stationary coordinates x_i that are aligned with the moving coordinates when source time τ is equal to zero.

The unsteady thickness noise generated by the interaction of the airfoil with the gust is given[1] by

$$p(x_i,t)=\frac{1}{4\pi}\frac{\partial^2}{\partial t\,\partial x_\beta}\int_\Sigma\left[\frac{\rho_0 h w_\beta}{r|1-M_r|}\right]d\Sigma \qquad \beta=1,2 \qquad (1)$$

where h is the thickness distribution, w_β the unsteady velocity components in the plane of motion, and Σ the blade planform. The rest of the notation is the same as in Ref. 1.

It is convenient to introduce another set of coordinates (α,ζ,κ), where α lies normal to the boundary of the moving fluid and ζ lies parallel to the boundary. Then the in-plane gust can be specified as

$$w_\beta=-\Delta V_\beta H(\alpha) \qquad \beta=1,2$$

where $\Delta V_1=\Delta V\cos\Theta$ and $\Delta V_2=\Delta V\sin\Theta$, and $H(\alpha)$ is the Heavyside function, equal to zero when $\alpha<0$ and unity when $\alpha>0$. The α coordinate can be related to the blade-based coordinates y_i through

$$\alpha=y_2\cos\Theta-(y_1-U\tau)\sin\Theta$$

where τ is source time and is related to observer time t using the far-field approximation

$$\tau=[t-(r_0/c_0-x_i y_i/r_0 c_0)](1-M_r)^{-1}$$

and $r_0=|x_i|$. Hence, α may be redefined in terms of observer time as

$$\alpha=y_2(\cos\Theta+\gamma\sin\Theta)-y_i\sin\Theta/(1-M_r)+U\tau_0\sin\Theta$$

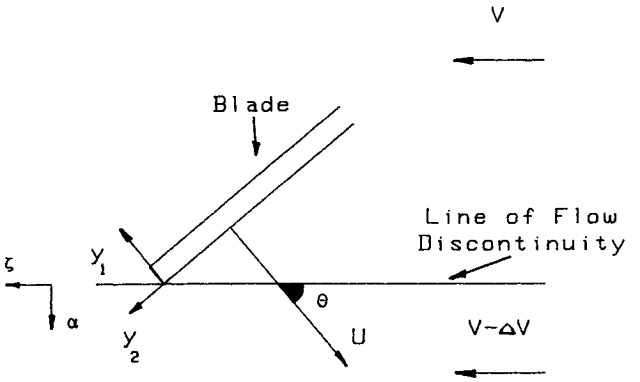

Fig. 1 Semi-infinite blade moving over a boundary separating two flows moving at different velocities. The deficit in the flow velocity is ΔV and the blade velocity is U.